P2Y2 receptor activation inhibits the expression of the sodium-chloride cotransporter NCC in distal convoluted tubule cells

Gailly, P ; Szutkowska, M ; Olinger, E ; Debaix, H ; Seghers, F ; Janas, S ; Vallon, V ; Devuyst, O

Abstract: Luminal nucleotide stimulation is known to reduce Na(+) transport in the distal nephron. Previous studies suggest that this mechanism may involve the thiazide-sensitive Na(+)-Cl(-) cotransporter (NCC), which plays an essential role in NaCl reabsorption in the cells lining the distal convoluted tubule (DCT). Here we show that stimulation of mouse DCT (mDCT) cells with ATP or UTP promoted Ca(2+) transients and decreased the expression of NCC at both mRNA and protein levels. Specific siRNA-mediated silencing of P2Y2 receptors almost completely abolished ATP/UTP-induced Ca(2+) transients and significantly reduced ATP/UTP-induced decrease of NCC expression. To test whether local variations in the intracellular Ca(2+) concentration ([Ca(2+)]i) may control NCC transcription, we overexpressed the Ca(2+)-binding protein parvalbumin selectively in the cytosol or in the nucleus of mDCT cells. The decrease in NCC mRNA upon nucleotide stimulation was abolished in cells overexpressing cytosolic PV but not in cells overexpressing either a nuclear-targeted PV or a mutated PV unable to bind Ca(2+). Using a firefly luciferase reporter gene strategy, we observed that the activity of NCC promoter region from -1 to -2,200 bp was not regulated by changes in [Ca(2+)]i. In contrast, high cytosolic calcium level induced instability of NCC mRNA. We conclude that in mDCT cells: (1) P2Y2 receptor is essential for the intracellular Ca(2+) signaling induced by ATP/UTP stimulation; (2) P2Y2-mediated increase of cytoplasmic Ca(2+) concentration down-regulates the expression of NCC; (3) the decrease of NCC expression occurs, at least in part, via destabilization of its mRNA.

DOI: https://doi.org/10.1007/s00424-013-1438-2

$P2Y_2$ Receptor Activation Inhibits the Expression of the Sodium-Chloride Cotransporter NCC in Distal Convoluted Tubule Cells.

P. Gailly[1*], M. Szutkowska[2 *], E. Olinger[2], H. Debaix[2], F. Seghers[1], S. Janas[2], V. Vallon[3] and O. Devuyst[2]

(1) Laboratory of Cell Physiology, Université catholique de Louvain (UCL) Medical School, Brussels, Belgium. (2) Division of Nephrology, Université catholique de Louvain (UCL) Medical School, Brussels, Belgium and Institute of Physiology and Mechanisms of Inherited Kidney Disorders Group, University of Zurich, Switzerland. (3) Department of Medicine, Division of Nephrology/Hypertension, University of California San Diego and VA San Diego Healthcare System, San Diego, USA.

* These authors contributed equally to this work

Correspondence: to Prof. Dr. O. Devuyst
University of Zurich, Institute of Physiology,
Mechanisms of Inherited Kidney Disorders Group,
Winterthurerstrasse, 190
CH-8057 Zürich
Phone: +41 (0)44 635 50 82; Fax: +41 (0)44 635 68 14
e-mail: olivier.devuyst@uzh.ch
or to Prof. Ph. Gailly
Laboratory of Cell Physiology, Université Catholique de Louvain, Avenue Hippocrate, B1.55.12, 1200 Brussels, Belgium. Tel.: 32-2-764-55-42; Fax: 32-2-764-55-80; e-mail: philippe.gailly@uclouvain.be.

Abstract

Luminal nucleotide stimulation is known to reduce Na^+ transport in the distal nephron. Previous studies suggest that this mechanism may involve the thiazide-sensitive Na^+-Cl^- cotransporter (NCC), which plays an essential role in NaCl reabsorption in the cells lining the distal convoluted tubule (DCT). Here we show that stimulation of mouse DCT (mDCT) cells with ATP or UTP promoted Ca^{2+} transients and decreased the expression of NCC at both mRNA and protein levels. Specific siRNA-mediated silencing of $P2Y_2$ receptors almost completely abolished ATP/UTP-induced Ca^{2+} transients and significantly reduced ATP/UTP-induced decrease of NCC expression. To test whether local variations in the intracellular Ca^{2+} concentration ($[Ca^{2+}]_i$) may control NCC transcription, we overexpressed the Ca^{2+}-binding protein parvalbumin selectively in the cytosol or in the nucleus of mDCT cells. The decrease in NCC mRNA upon nucleotide stimulation was abolished in cells overexpressing cytosolic PV but not in cells overexpressing either a nuclear-targeted PV or a mutated PV unable to bind Ca^{2+}. Using a firefly luciferase reporter gene strategy, we observed that the activity of NCC promoter region from -1 to -2200 bp was not regulated by changes in $[Ca^{2+}]_i$. In contrast, high cytosolic calcium level induced instability of NCC mRNA. We conclude that in mDCT cells: (1) $P2Y_2$ receptor is essential for the intracellular Ca^{2+} signaling induced by ATP/UTP stimulation; (2) $P2Y_2$-mediated increase of cytoplasmic Ca^{2+} concentration downregulates the expression of NCC; (3) the decrease of NCC expression occurs, at least in part, via destabilization of its mRNA.

Keywords

Distal convoluted tubule, mDCT cells, P2 receptor signaling, cytosolic calcium level, post transcriptional modifications.

Abbreviations

ATP/UTP, Adenosine-5'-triphosphate / Uridine-5'-triphosphate; $[Ca^{2+}]_e$, extracellular Ca^{2+} concentration; $[Ca^{2+}]_i$, intracellular Ca^{2+} concentration; DCT, distal convoluted tubule; mDCT, mouse DCT; EGTA-AM, Ethylene glycol tetra (acetoxymethyl ester); FITC, fluorescein isothiocyanate; GAPDH, Glyceraldehyde 3-phosphate dehydrogenase; NCC, Na^+-Cl^- cotransporter; nCaRE, negative calcium response element; PLC, Phospholipase C; PV, parvalbumin; TRPM6, transient receptor potential cation channel, subfamily M, member 6.

Introduction

The strict control of NaCl excretion by the kidney is essential for maintaining body fluid homeostasis as well as blood pressure. The distal convoluted tubule (DCT) reabsorbs 5 to 10% of the filtered Na^+, via the thiazide-sensitive Na^+-Cl^- cotransporter (NCC), located on the apical membrane. NCC is phosphorylated and activated by WNK via specific SPAK isoforms that are expressed in the DCT [9]. The functional importance of NCC is illustrated by Gitelman syndrome, an autosomal recessive tubulopathy characterized by salt wasting and secondary aldosteronism responsible for hypokalemia and metabolic alkalosis, and by hypomagnesemia and hypocalciuria [13]. Gitelman syndrome is most often due to invalidating mutations in the *SLC12A3* gene that codes for NCC [45].

Recently, we provided *in vitro* and *in vivo* evidence that NCC expression was modulated by the presence of parvalbumin (PV), a cytosolic "EF-hand" protein able to bind divalent cations and specifically expressed in early DCT (DCT1) [4]. The fact that DCT segment as well as immortalized mouse DCT cell line (mDCT) that expresses NCC and other typical markers were sensitive to nucleotide stimulation, known to induce Ca^{2+} signaling, led us to hypothesize that NCC expression might be controlled by ATP/UTP-induced Ca^{2+} transients [4,8].

Response to ATP and UTP involves nucleotide P2 receptors. Seven ionotropic P2X (P2X1-7) and five metabotropic P2Y (P2Y1, -2,-4, -6 and -11) receptors have been identified in the kidney, each with a specific agonist response profile (for review see refs [23,43,44]). Several P2Y receptor subtypes are coupled to G-protein subtype $G\alpha_q$, which activates PLC-β and promotes mobilization of Ca^{2+} from intracellular stores. One of them, the $P2Y_2$ receptor, which is activated by both ATP and UTP, has previously been linked to electrolyte and water transport processes in the kidney (for review [44]). Indeed, in the intact mouse collecting duct, luminal ATP/UTP stimulation via $P2Y_2$-like receptors inhibits electrogenic Na^+ transport and decreases K^+ secretion, thus inhibiting transport processes for salt and water absorption in this nephron segment [22,23,25]. Making use of $P2Y_2$ receptor knockout mice, it was subsequently shown that this receptor contributes to blood pressure regulation, and renal fluid and NaCl reabsorption by inhibitory effects on the expression of the Na-2Cl-K cotransporter NKCC2 and the water channel aquaporin-2 [33]. These studies further showed that local $P2Y_2$ receptor tone in the aldosterone-sensitive distal nephron exerts paracrine downregulation of epithelial sodium channel (ENaC) activity by lowering channel open probability [30],

and that this mechanism explains the inhibition of ENaC activity following an increase in dietary NaCl intake and contributes to blood pressure regulation [31]. The precise role of P2Y receptors in the DCT is however not yet characterized.

In the present study, we aimed at identifying the P2 receptors involved in Ca^{2+} signaling in DCT and how the nucleotide stimulus could regulate the NCC expression in the mDCT cells. We show that the $P2Y_2$ receptor is present in DCT cells and that it is the main functional receptor, essential for the intracellular Ca^{2+} signaling induced by extracellular ATP/UTP in mDCT cells. $P2Y_2$ stimulation induces cytosolic Ca^{2+} transients, regulating the NCC expression by decreasing the stability of its mRNA.

Methods

Cell culture.

The immortalized mDCT cell line was kindly provided by Prof. P. A. Friedman (University of Pittsburgh School of Medicine, Pittsburgh, PA). mDCT cells have been previously characterized as a model for thiazide-sensitive Na^+ and Ca^{2+} transport occurring in the DCT and they express sizeable endogenous NCC as well as other markers of the DCT1 [12]. Cells were grown in DMEM/Ham's F12 medium (Lonza, Verviers, Belgium) supplemented with 5% (v/v) fetal bovine serum (Lonza), 2mM ultraglutamine (Lonza) and a mixture of penicillin/streptomycin (Invitrogen, Carlsbad, CA) in a humidified atmosphere of 5% (v/v) CO_2 at 37°C. Studies were performed in 24-well plates between passages 25 and 35.

Drug treatments.

During nucleotide stimulation experiments, confluent cells were treated with either ATP (Boehringer Mannheim, Roche Applied Science) or UTP (Sigma-Aldrich) at different concentrations (1, 5, 10, 50 or 100 µM). For repetitive stimulations protocol, cells were stimulated with ATP or UTP 10 µM for 10 min, then rinsed (to avoid receptor down-regulation) and re-stimulated every hour, for 6 h. To suppress phospholipase C (PLC) activity, cells were treated with 10 µM of the PLC inhibitor U73122 (Tocris, Bioscience), 10 min before Ca^{2+} measurements. In mRNA stability experiments, the transcriptional inhibitor 6-dichloro-1-b-ribofuranosylbenzimidazole (DRB, Sigma) was used at 75 µM throughout the duration of the experiment.

Transient transfections.

Subconfluent cultures (approximately 80%) were transfected using Lipofectamine™ 2000 (Invitrogen) with pCMV-GFP (Mock), pCMV-PV-cyto-GFP (PV-cyto) or pCMV-PV-nuc-GFP (PV-nuc) plasmids (Addgene, Cambridge, USA).

Site-directed mutagenesis was carried out to generate the mutant PV plasmid pCMV-PV-cyto-CDEF-GFP coding for PV in which both functional Ca^{2+}-binding sites were inactivated by substituting a glutamate for a valine residue at position 12 of each Ca^{2+}-binding loop. The mutant construct was generated by using pCMV-PV-cyto-GFP plasmid as a template and by using the QuickChange® Lightning Site-Directed Mutagenesis Kit (Stratagene, Agilent) following the manufacturer's protocol. Mutant

plasmid was generated by polymerase chain reaction using the following synthetic oligonucleotides containing mismatches in codon 62 of the CD loop and in codon 101 of the EF loop were used: CD_{62}: 5'-TTCATTGAGGAGGATGTGCTGGGGTCCATTCTG-3', and EF_{101}, 5'-GCAAGATTGGGGTTGAAGTGTTCTCCACTCTGGTGGCC-3' (mutated nucleotides are underlined). We checked the identity of the mutant plasmid by sequencing.

RNA Interference.

To knockdown the endogenous *p2ry2* expression, a pool of 3 different double-strand siRNAs (15nM, *Silencer*^{R} Select Pre-designed siRNA synthesized by Ambion) was introduced into mDCT cells using Lipofectamine^{TM} RNAiMAX (Invitrogen). Cells were cultured on plate wells containing the transfection complexes. Seventy-two hours after transfection, RNA was extracted with RNAqueous^{R}-Micro kit and subjected to real-time PCR. Transfection efficiency was assessed using BLOCK-iT^{TM} Alexa Fluor^{R} Red Fluorescent Oligo (Invitrogen). Fluorescent siRNAs were used to follow transfection in fluorescence microscopy.

Extraction of RNA, quantitative RT-PCR.

mDCT mRNAs were extracted with RNAqueous^{R}-Micro kit (Ambion, Invitrogen)) and reversed-transcribed using iScript ^{TM} cDNA Synthesis Kit (Bio-Rad). Gene-specific PCR primers were designed using Primer3 [35] (See Table 1). Total RNA samples were stored at -80°C. Real-time RT-PCR was performed using 1 µg cDNA, 10 µl of SybrGreen Mix (BioRad) and 100 nM of each primer in a total reaction volume of 20 µl. PCR conditions were 95°C for 3 min followed by 40 cycles of 15 sec at 95°C, 30 sec at 60°C. The PCR products were sequenced with the BigDye terminator kit (Perkin Elmer Applied Biosystems). The multiScreen SEQ_{384} Filter Plate (Millipore, Billerica, USA) and Sephadex G-50 DNA Grade Fine (Amersham Biosciences, Piscataway, USA) dye terminator removal were used to purify sequences reactions before analysis on an ABI3100 capillary sequencer (Perkin Elmer Applied Biosystems).

The efficiency of each set of primers was determined by dilution curves (Table 1).

Each cDNA was amplified in duplicate and cycle threshold values (Ct) were averaged for each duplicate. The average Ct value for GAPDH was subtracted from the average Ct value for the gene of interest. This ΔCt value determined in specific experimental conditions, was then subtracted from the ΔCt value determined in control conditions to

obtain a ΔΔCt value. As amplification efficiencies of the genes of interest and GAPDH were comparable, the amount of mRNA, normalized to GAPDH, was given by the relation $2^{-\Delta\Delta Ct}$ [7,24].

Semiquantitative RT-PCR.

We used RT-PCR to assess the presence of P2X and P2Y receptors in microdissected nephron segments. PCR conditions used were: 94°C for 3 min followed by 35 cycles of 30 sec at 95°C, 30 sec at 60°C and 1 min at 72°C with FastStart Taq polymerase (Roche, Vilvoorde, Belgium). The PCR products were separated on a 2% agarose gel.

$[Ca^{2+}]_i$ measurements.

mDCT cells were cultured on coverslips until they reached 70% confluence. Cell cultures were incubated with 1μM Fura2-AM for 60 min at room temperature, prior to the measurement of fluorescence in individual cells. Coverslips were rinsed with Krebs medium containing (mM): 135 NaCl, 5.9 KCl, 1.8 CaCl, 1.2 $MgCl_2$, 11.6 Hepes and 10 glucose, (pH 7.3) for 30 min and mounted in a thermostatized (20°C) chamber. The chamber was continuously superfused (1 ml/min, or 4 ml/min for quick exchanges of solutions).

Cytosolic concentration of free Ca^{2+} was measured at room temperature by radiometric measurements of fluorescence intensity monitored at 510 nm [11]. Fura-2 loaded cells were excited alternatively at 340 and 380 nm and fluorescence emission was monitored at 510 nm using a Deltascan spectrofluorimeter (Photon Technology International) coupled to an inverted microscope (Nikon Diaphot, oil immersion objective 40X N.A. 1.3). Fluorescence intensity was recorded over the entire surface of the single cells. $[Ca^{2+}]_i$ was calculated from the ratio of the fluorescence intensities excited at the two wavelengths, using a standard intracellular calibration procedure performed after cell permeabilization with 5 μM ionomycin. In Ca^{2+}-free solution, $CaCl_2$ was omitted and 0.2 mM EGTA (Molecular Probes, Invitrogen) was added. In the experiments designed to investigate the role of PV in $[Ca^{2+}]_i$ responses, $[Ca^{2+}]_i$ measurements were performed only on cells expressing PV-GFP plasmids (cells selected by GFP fluorescence).

Antibodies.

The rabbit anti-$P2Y_2$ (Abcam: ab 46537), rabbit anti-NCC [39], goat anti-PV (Santa Cruz Biotechnology, Inc: sc-7448) and mouse anti β-actin (Sigma-Aldrich Corporation)

primary antibodies were used during experiments. To visualize, secondary fluorescent antibody: Alexa Fluor (647 anti-rat, 633 anti-rabbit, 633 anti-sheep, 488 anti-goat and 488 anti-rabbit) were used for immunofluorescent assays (Molecular Probes).

Immunoblotting.

Total membrane -and cytosolic proteins extracts were prepared from mDCT cells after homogenization with a Tissue Tearor Homogenizer. The lysis buffer contained 250 mM sucrose, 20 mM imidazole pH 7.2, 1 mM EDTA and a protease inhibitors mix Complete (Roche). The sample (total extract) was centrifuged at 1000 g for 15 min at 4°C for nucleus elimination. The supernatant was then centrifuged at 38500 rpm for 120 min at 4°C. The pellet (membrane extract) was suspended in 300 µl of lysis buffer. The supernatant contains the cytosolic fraction. Protein concentrations were determined with the bicinchoninic acid assay using BSA as standard. Membrane proteins were solubilized 1/4 in sample buffer (50 mM Tris-HCl, pH 6.8, 7.5% SDS, 30% glycerol, 0.004% bromophenol blue) containing 6% of DTT and heated at 95°C for 5 min.

SDS-PAGE was performed under reduced conditions. For western blotting, 40 µg of protein was loaded onto a SDS-polyacrylamide gel and separated by electrophoresis. After blotting on nitrocellulose, the membranes were incubated overnight at 4°C with primary antibodies, washed and incubated for 1 h at room temperature with peroxidase-labeled antibodies (Dako). Secondary antibodies conjugated to horseradish-peroxidase were detected with ECL reagent (Amersham Biosciences). The molecular weight of proteins was estimated by running the Precision Plus Protein^{TM} All Blue standard (Bio-Rad).

Immunostaining.

Cell cultures were grown on permeable filter supports until confluence. 24 hours before cell fixation, standard culture medium was replaced by DMEM/F12 supplemented with REGM^{TM} Single Quots (Lonza). Cells were fixed 10 minutes using 4 % formaldehyde, washed three times with DPBS and permeabilized using 0.2% Triton X-100. Cells were then preincubated 1 hour with DPBS containing 3% blocking-serum, 1 h with primary antibodies at room temperature, 30 min with the secondary fluorescent antibodies and washed with DPBS before mounting with DAPI-ProLong^{R} Gold (Invitrogen). Sections were viewed with a Zeiss LSM 410 confocal microscope or Leica CLSM confocal microscope. Images were processed (overlays) using Adobe Photoshop.

mRNA half-life time determination.

mDCT cells were cultured up to 80% confluence and treated with 75 µM DRB for different time intervals. NCC, β-actin and TRPM6 expressions were measured using RT-qPCR. mRNA half-life time was estimated by exponential regression analysis [34].

Plasmid construction for reporter assay.

The plasmid pGL3-basic (Promega) was used to examine the promoter activity of the 5'-flanking region in the mouse *Slc12a3* gene. The 5'-flanking region of *Slc12a3* was generated by PCR and ligated into *KpnI* and *XhoI* sites of pGL3-basic vector. Sense primer: 5' Ttggtacc GTGCCATCCTTCCTCATTCC 3' (nucleotide -1502) containing an engineered *KpnI* restriction site was derived from the Slc12a3 gene sequence, and the antisense primer: 5' Ttctcgag TATGGCTCTGGGTATCAAAGG 3' was corresponding to nucleotides -1 to -21 and containing an engineered *XhoI* restriction site. Construct (pGL3-1500/Slc12a3) was confirmed by sequence analysis. The pGL3-1000/Slc12a3 was generated with Sense primer: Ttggtacc GATGATTCAGGGAAACACTGG 3'(nucleotide -1015) and the antisense primer was the same than for pGL3-1500. The pGL3-2200/Slc12a3 was constructed by PCR amplification using an engineered *KpnI* restriction site in the Sense primer: 5'TtggtaccAGAGTCCCACCA 3' corresponding to nucleotide -2246 and the antisense primer: 5' AagcatgcTACTTGGCTATCAA (nucleotide -1274). The *Slc12a3* gene sequence contained a restriction site for *SphI* in position -1280. PCR fragment was then ligated into the pGL3-1500/Slc12a3 plasmid digested with *KpnI* and *SphI* restriction enzymes to generate pGL3-2200/Slc12a3 plasmid.

Plasmids were sequenced with the BigDye terminator kit (Perkin Elmer Applied Biosystems). The multiScreen SEQ_{384} Filter Plate (Millipore, Billerica, USA) and Sephadex G-50 DNA Grade Fine (Amersham Biosciences, Piscataway, USA) dye terminator removal were used to purify sequences reactions before analysis on an ABI3100 capillary sequencer (Perkin Elmer Applied Biosystems).

Luciferase assay.

mDCT were transiently transfected with 500ng firefly luciferase reporter plasmid and 10ng *Renilla* luciferase vector using Lipofectamine 2000 (Invitrogen).

Forty-eight hours after transfection, luciferase activity was measured with Dual-Luciferase Reporter Assay System (Promega), using a GloMax™ 96 luminometer (Promega) with a 10-second integration time for each luciferase reaction. Firefly luciferase activity was corrected for transfection efficiency by using *Renilla* luciferase measurements. The corrected activity (Firefly luciferase divided by *Renilla* luciferase activity) was compared to the promoterless pGL3-basic corrected activity, used as a negative control (results expressed as percentages).

Extracts from each transfection were assayed in duplicate for at least 3 independent transfection experiments.

Statistical Analysis.

The results are presented as means ± SEM. One-way analysis of variance was used to investigate statistical differences among the studied groups. Individual groups were compared by an unpaired Student's *t test*. A p value of < 0.05 was taken as significant.

Results

1. Stimulation of mDCT cells by ATP and UTP decreases NCC mRNA level.

Based on our previous observation that Ca^{2+} signaling regulates the expression of NCC in mDCT cells [4], we first investigated whether the nucleotides ATP and UTP, known to trigger changes in intracellular free calcium concentration ($[Ca^{2+}]_i$), regulate the mRNA expression of NCC. mDCT cells were treated with ATP or UTP 10µM for 10 min every hour for 6h. Both treatments produced a significant decrease in NCC mRNA level compared to control (59 ± 12% and 58 ± 7% respectively, n=8, Fig. 1A). We also observed that the effect on NCC expression obtained at this concentration (10 µM ATP / UTP) was maximal (data not shown). Accordingly, repetitive stimulation with 10 µM UTP for 10 min every hour for 6h decreased the amount of NCC protein expressed after 24 h by ~40 % (Fig. 1A insert).

2. *ATP and UTP increase $[Ca^{2+}]_i$ in mDCT cells.*

The involvement of P2 receptors was further characterized in mDCT cells by analyzing $[Ca^{2+}]_i$ transients after ATP and UTP stimulation. mDCT cells were loaded with the calcium indicator fura-2 acetoxymethyl ester (Fura-2 AM) to measure $[Ca^{2+}]_i$. In the presence of Ca^{2+} in the extracellular medium, the response was constituted of a fast peak of $[Ca^{2+}]_i$ followed by a sustained plateau (Fig. 1B a). The response was largely inhibited by suramine (300 µM) suggesting the involvement of a P2 receptor (data not shown). In the absence of external Ca^{2+}, ATP was still able to induce the fast initial peak of $[Ca^{2+}]_i$, but the long lasting plateau phase was lost, suggesting that ATP stimulation triggers both the release of Ca^{2+} from internal stores and the entry of Ca^{2+} from the external milieu (Figs. 1B a-b). This also suggested that the purinergic receptor involved in the first phase is metabotropic, belonging to the P2Y family [4]. UTP elicited a similar increase in $[Ca^{2+}]_i$ as observed for ATP and exerted a maximal effect at 10 µM (Figs. 1B c-d). We further characterized the presence of functional P2Y receptors coupled to Gq protein by testing the effect of the phospholipase C (PLC) antagonist, U73122 (10 nM), on $[Ca^{2+}]_i$ response elicited by ATP/UTP. U73122 completely inhibited the increase in $[Ca^{2+}]_i$, both in the presence and in the absence of external Ca^{2+} (Figs. 1B a-c) confirming that the receptor involved is metabotropic and coupled to PLC, and suggesting that the entry of Ca^{2+} is not due to P2X receptor stimulation but is

subsequent to stores depletion. Taken together, these observations indicate that mDCT cells express functional P2Y receptor subtypes sensitive to ATP and UTP.

3. *mDCT cells express P2Y2 receptor in cell membrane.*

Among P2Y and P2X receptors, $P2Y_1$, $P2Y_2$, $P2Y_4$, $P2Y_6$ and $P2X_{1\text{-}7}$ subtypes have been previously identified in kidney [1,23,36,41,42]. Semiquantitative (Fig. 1C a) and quantitative (Table 1) RT-PCR experiments showed that $P2Y_1$, $P2Y_2$ and $P2Y_6$ as well as $P2X_4$ and $P2X_5$ were by far the most expressed subtypes in mDCT cells.

Immunofluorescent microscopy was used to study subcellular localization of the $P2Y_2$ receptor subtype in mDCT cells (see the reason below). As expected, the $P2Y_2$ receptor was found in the membrane compartment whereas parvalbumin (PV), a specific marker of DCT1, was found in the cytosol (Fig. 1C b).

4. *$P2Y_2$ receptor silencing suppresses nucleotide-induced increases in $[Ca^{2+}]_i$ and suppression of NCC expression.*

The similar and high potency of both ATP and UTP in the above studies pointed to a possible role of the P2Y2 and/or P2Y4 receptor, which in rodents are both and similarly activated by both nucleotides, whereas P2Y1 and P2Y6 subtypes are not responsive to UTP and ATP, respectively. To identify the P2Y receptor involved in the described response in mDCT cells and considering the high expression of $P2Y_2$ versus $P2Y_4$ receptors in mDCT cells, we repressed the expression of the $P2Y_2$ receptor. mDCT cells were transfected with nonspecific siRNA (siCtrl) or treated independently with three specific siRNAs targeted against $P2Y_2$ receptor ($siP2Y_2$). Treatment with $siP2Y_2$ resulted in a significant reduction of about 80% in $P2Y_2$ mRNA levels, with no effect on the $P2Y_1$ mRNA level (Fig. 2A a). Accordingly, 72h after transfection with a pool of the three $siP2Y_2$, Western blot analysis revealed a strong reduction in the $P2Y_2$ receptor protein expressed (Fig. 2A b).

We then observed that in mDCT cells transfected with this pool of three siP2Y2, the Ca^{2+} response to nucleotide stimulation (10 µM UTP) was completely abolished, emphasizing the essential involvement of $P2Y_2$ receptors in nucleotide-induced release of $[Ca^{2+}]_i$ (Fig. 2B).

We previously reported that the ATP-induced decrease in NCC expression was dependent on intact $[Ca^{2+}]_i$ transients [4]. We therefore used the same siRNA strategy to determine the role of $P2Y_2$ receptor signaling in the nucleotide-induced regulation of

NCC expression. Compared to baseline conditions, $P2Y_2$ receptor knock-down prevented the decrease in NCC expression induced by nucleotide activation (10 µM UTP) (Fig. 2C).

Altogether, these observations indicate that $P2Y_2$ receptors mediate the $[Ca^{2+}]_i$ transients and the negative regulation of NCC expression induced by extracellular nucleotides.

5. Selective cytoplasmic Ca^{2+} buffering prevents the nucleotide-induced decrease of NCC mRNA expression.

We next investigated the relative role of localized $[Ca^{2+}]_i$ transients (nuclear vs. cytoplasmic) in nucleotide-induced regulation of NCC expression. To this aim, we overexpressed PV specifically in the cytosol or in the nucleus. mDCT cells were transfected with plasmids coding for rat PV targeted to the cytosol (PV-cyto) and rat PV targeted to the nucleus (PV-nuc), respectively [32]. We used, as controls, a plasmid coding GFP alone (Mock) and a plasmid coding for a mutated form of PV in which both calcium binding sites were rendered nonfunctional (PV-cyto-CDEF). These proteins were built as GFP-fusion proteins and their proper targeting confirmed by fluorescent detection (Fig. 3 A).

At rest, cells transfected with PV-cyto, PV-cyto-CDEF or PV-nuc did not show any significant difference in $[Ca^{2+}]_i$ in comparison to Mock transfected cells. However, UTP-induced cytosolic $[Ca^{2+}]_i$ transients were largely reduced in PV-cyto transfected cells compared to control Mock transfected cells (274 ± 42 nM vs. 755 ± 71 nM). As expected, overexpression of PV in the nucleus and overexpression of the mutated PV unable to bind Ca^{2+} did not affect the UTP-induced $[Ca^{2+}]_i$ response (824 ± 43 nM and 826 ± 62 nM, respectively) (Fig. 3B).

Having validated the experimental model, we investigated the effect of local changes in $[Ca^{2+}]$ on the regulation of NCC expression. UTP stimulation of Mock as well as PV-cyto-CDEF and PV-nuc transfected cells induced a significant decrease in NCC expression. In contrast, buffering of cytoplasmic Ca^{2+} by overexpression of PV-cyto completely inhibited the effect (Fig. 3C), suggesting that an increase of cytosolic but not of nuclear $[Ca^{2+}]$ inhibits NCC expression. This also suggests that if Ca^{2+} exerts its effects on NCC expression by acting on transcription, it is not a direct effect of Ca^{2+} on the promoter but an indirect effect passing through a cytosolic factor.

6. Nucleotide stimulation does not influence NCC gene transcription.

To evaluate whether nucleotide stimulation could interfere with NCC transcription, we measured the activity of NCC gene promoter using a firefly luciferase reporter gene. As it has been reported that maximal activity of the promoter requires a sequence of 1019 bp for human and of 2,1 kb for rat [41], mDCT cells were transfected with three Slc12a3 promoter-luciferase gene constructs containing a sequence of the promoter of 1, 1.2 and 1.5 kb, respectively (pGL3-1000/SLC12a3, pGL3-1500/Slc12a3 and pGL3-2200/Slc12a3, repectively). Red firefly luciferase activity was corrected for transfection efficiency by measuring the activity of the simultaneously transfected green *Renilla* luciferase. Firefly luciferase activities measured in cells transfected with pGL3-1000/Slc12a3, pGL3-1500/Slc12a3 and pGL3-2200/Slc12a3 were significantly higher than in cells transfected with the control vector (pGL3-basic), suggesting that the constructs were transcriptionally active. Treatment of the cells with 10 µM UTP for 10 min every hour for 6h did not reduce the expression of luciferase, suggesting that the activity of the NCC promoter region from -1 to -2200 bp is not regulated by nucleotide stimulation (Fig. 4). These results argued against important regulatory sequences for nucleotide-induced and Ca^{2+}-mediated inhibition of NCC gene transcription in the area of the NCC promoter.

7. Nucleotide stimulation decreases NCC mRNA stability.

Since UTP-induced decrease of NCC expression seemed independent of transcription, we checked whether UTP might interfere with mRNA stability. To this aim, we blocked transcription with 75 µM of DRB and measured the progressive decay of mRNA amount by RT-qPCR. Analysis showed that NCC mRNA half-life time significantly decreased upon UTP stimulation, from 11.2h to 5.9h (Fig. 5). In comparison, nucleotide stimulation did not affect the relative half-life time of other genes such as β-actin or the magnesium transporter TRPM6 (10h and 10.3h, respectively). We conclude that UTP stimulation specifically decreases NCC mRNA stability in mDCT cells.

Discussion

We previously reported that ATP stimulation of mDCT cells significantly reduced NCC expression [4]. In the present study, we investigated how ATP-induced Ca^{2+} signaling regulates NCC expression and elucidated the involved P2 receptor subtype. We show that $P2Y_2$ receptor plays an essential role in this response, which is induced by both ATP and UTP. We further show that the ATP/UTP-induced increase in cytoplasmic Ca^{2+} concentration downregulates the expression of NCC, at least in part, by decreasing its mRNA stability.

The DCT segment is not readily accessible by regular microdissection of the mouse kidney. Therefore, most receptor studies of the distal tubule have been performed thus far on cell lines. Nucleotide receptors have been studied on *Xenopus laevis* A6, canine MDCK and rabbit DC1 cells [2,5,46]. Here, we used mDCT cells, an established cell model that expresses the thiazide-sensitive cotransporter NCC typical for the DCT [12] and which has recently been used to study the regulation of NCC and the expression of other DCT1 markers such as parvalbumin [4].

Cytosolic ATP concentrations exceed 5mM in most cell types [14,19], whereas the pericellular concentrations required for $P2Y_2$ receptor stimulation (EC_{50} values for ATP) range between 0.085 µM and 0.23 µM in humans and 0.7 µM and 1.8 µM in mice. Similar concentrations are necessary for activation of this receptor by UTP [38]. Lazarowski and colleagues detected UTP in nanomolar concentrations in the medium bathing a variety of cells including platelets and leukocytes, primary airway epithelial cells, rat astrocytes and several cell lines cultures [20]. This suggests that constitutive release of UTP may provide a mechanism of regulation of the basal activity of uridine nucleotide sensitive receptors. Interestingly, high dietary NaCl intake is paralleled by increased urinary levels of UTP and ATP. Such change in NaCl intake, reflected by modifications in aldosterone concentration, may change $P2Y_2$-receptor activation, in turn affecting ENaC open probability and therefore NaCl reabsorption [31].

Extracellular nucleotides can activate two families of receptors: i) The ionotropic P2X receptors that open in response to the binding of extracellular ATP as their principal ligand [6]; and (ii) the metabotropic P2Y receptors that are functionally coupled to G proteins [44] and that are activated by ATP ($P2Y_1$ and $P2Y_2$ receptors) or UTP ($P2Y_2$, $P2Y_4$ and $P2Y_6$ receptors) [21,44]. By RT-qPCR, we identified the presence of several subtypes of P2Y and P2X receptors among which $P2Y_1$, $P2Y_2$, $P2Y_6$, $P2X_4$

and $P2X_5$ were the most highly expressed. ATP and UTP induced an increase in $[Ca^{2+}]_i$ even in the absence of extracellular calcium (0 mM $[Ca^{2+}]_e$), suggesting the involvement of metabotropic receptors. Accordingly, the PLC antagonist U73122 inhibited the ATP/UTP-elicited calcium peak in mDCT cells. Among the P2Y metabotropic receptors, the similar and high potency of ATP and UTP suggested the possible involvement of $P2Y_2$ in mDCT cells, which was highly expressed in these cells. siRNA-mediated knock-down of $P2Y_2$ receptor protein confirmed that this isoform was responsible of both ATP/UTP-induced $[Ca^{2+}]_i$ transients and ATP/UTP-induced inhibition of NCC expression. $P2Y_2$ receptor and NCC (the latter not shown) were immunodetected in the apical membrane of the mDCT cells cultivated on filter whereas PV, a protein specifically expressed in mouse DCT1, was found in the cytosol. $P2Y_2$ has also been described in both apical and basolateral membranes of principal cells of the inner medullary collecting duct (IMCD) [17,42,44].

Our understanding of the distinct roles of cytosolic and nuclear Ca^{2+} transients in gene expression is still limited. The generation of PV expression constructs targeted to the cytosol or to the nucleus allowed to investigate the relative contribution of cytoplasmic and nuclear Ca^{2+} transients to the regulation of MAPK-mediated gene expression in response to stimulation with EGF [32]. We used the same strategy and found that cytosolic and not nuclear Ca^{2+} transients played a decisive role in the regulation of NCC expression. This observation was confirmed by the fact that the expression of neither the mutated PV unable to bind Ca^{2+} nor the nuclear-targeted PV were able to inhibit UTP-induced modulation of NCC expression. Taken together with the specific buffering properties of PV [29], these data suggest that the calcium signal peak is indeed the determinant factor for NCC regulation.

Gene expression may be regulated at the level of RNA transcription, splicing, polyadenylation, capping, trafficking, stability, translation, or at the level of protein processing and stability [27]. Genes down-regulated by Ca^{2+} transients have been identified in *Arabidopsis*, but also in mammals [15,16]. For example, it was shown that Ca^{2+} transients inhibit expression of the protooncogene *c-myb* in an erythropoietin-responsive murine erythroleukemia cell line [37]. Similarly, calcium inhibits renin gene expression by transcriptional and posttranscriptional mechanisms [10]. It inhibits renin transcription by inducing translocation of transcription factor Ref-1 to the nucleus, where it binds to a negative calcium response element (nCaRE) of the renin promoter /

enhancer. Besides its indirect action on transcription, Ca^{2+} also induces a destabilization of renin mRNA, a process involving dynamin-1 protein [18].

In the present study, we showed that NCC mRNA levels decreased after UTP stimulation, suggesting that UTP stimulation inhibits NCC transcription or makes NCC mRNA less stable [34,36]. We therefore studied the role of UTP-induced Ca^{2+} transients in both these processes.

Maximal promoter activity of NCC was observed in mDCT cells using a human promoter containing 1019bp of the 5' flanking region of SLC12A3. MacKenzie and colleagues observed a significant repressor effect from position –1019 to –1885 [26]. Luciferase reporter gene analysis using the rat promoter sequence of SLC12A3 showed a maximal activity with a promoter containing 2039bp and demonstrated that the most important region was located between position –580 and –141 [41]. *In silico* analysis of NCC sequence did not reveal any nCaRE element in the promoter region. We nevertheless studied the possible effect of $[Ca^{2+}]_i$ transients on NCC gene transcription by using a firefly luciferase reporter gene using the rat promoter sequence up to 2.2 kb upward the start codon. Based on these observations in mDCT cells, it seems that nucleotide-stimulation, shown to increase intracellular Ca^{2+} concentrations, has no direct or indirect influence on NCC gene transcription. However, we cannot exclude a possible involvement of a region upstream this 2.2 kb sequence.

We next turned to mRNA stability investigation. Importantly, we found that repeated stimulations with 10 µM UTP (for 10 min every hour for 6 h), eliciting repeated pulses of high intracellular calcium concentrations, reduced NCC mRNA half-life by 50%. Messenger RNA stability is determined by specific sequences (*cis*-acting elements) in the 3'-UTR of RNA such as AUUUA, U(U/A)(U/A)UUU(u/A)(U/A)U, GUUUG or CAGUGU/C repeats and by the presence of specialized proteins (*trans*-acting factors) such as heterogeneous nuclear ribonucleoprotein-A1 (hnRNP-A1), a protein known to bind, in the cytoplasm, to reiterated AUUUA, AU-rich and poly-U sequences to determine mRNA stability [3,27]. We did not identify in a short 250b long 3'-UTR sequence of NCC the classical AU-rich elements (ARE) "AUUUA" motif typically responsible for the *trans*-acting factors binding. However, even though the "AUUUA" repeats are commonly involved in mRNA stability regulation, they are not essential. For example, parathyroid hormone mRNA is known to contain a 63b cis-acting nucleotide destabilizing AU-rich sequence in the 3'UTR and another distinct region determining mRNA stability by its interaction with trans-acting factors AUF-1 and Unr. Both

proteins bind PTH mRNA and stabilize the transcript; interestingly, their binding is increased in low $[Ca^{2+}]_i$ environment [28].

Finally, mRNA abundance could be regulated by binding of specific miRNAs to a complementary binding sequence generally located in 3'UTR of target RNA. In the case of murine NCC mRNA, a computational analysis of 3'UTR identified two potential sites of fixation for miRNA described in kidney: mmu-let-7d and mmu-miR-143. Recently, these miRNA were implicated in cancer protein regulation. The importance of 3'-UTR region in Ca^{2+}-induced destabilization of NCC mRNA and protein is under investigation.

In conclusion, our results demonstrate that in mDCT cells, the extracellular nucleotide-induced and $P2Y_2$ receptor-mediated $[Ca^{2+}]_i$ elevation is associated with a decrease in NCC mRNA, which is due, at least in part, to a reduction of its stability. These studies provide another example for the down-regulation of a mammalian gene by Ca^{2+} transients and add another level of complexity to the regulation of NCC expression in the distal nephron.

Acknowledgments

This study was supported by the Belgian agencies "Fonds National de la Recherche Scientifique" and "Fonds de la Recherche Scientifique Médicale", Concerted Research Action (10-15/029) and Inter-University Attraction Poles (IUAP P7/13) from the Belgian Federal Government and by the NCCR Kidney.CH program (Swiss National Science Foundation); the Gebert Rüf Stiftung (Project GRS-038/12); and the Swiss National Science Foundation 310030-146490 (to OD).

The authors have declared that no conflict of interest exists.

References

1. Bailey MA, Hillman KA, Unwin RJ (2000) P2 receptors in the kidney. Journal of the autonomic nervous system 81 (1-3):264-270
2. Banderali U, Brochiero E, Lindenthal S, Raschi C, Bogliolo S, Ehrenfeld J (1999) Control of apical membrane chloride permeability in the renal A6 cell line by nucleotides. The Journal of physiology 519 Pt 3:737-751
3. Beelman CA, Parker R (1995) Degradation of mRNA in eukaryotes. Cell 81 (2):179-183
4. Belge H, Gailly P, Schwaller B, Loffing J, Debaix H, Riveira-Munoz E, Beauwens R, Devogelaer JP, Hoenderop JG, Bindels RJ, Devuyst O (2007) Renal expression of parvalbumin is critical for NaCl handling and response to diuretics. Proceedings of the National Academy of Sciences of the United States of America 104 (37):14849-14854. doi:10.1073/pnas.0702810104
5. Bidet M, De Renzis G, Martial S, Rubera I, Tauc M, Poujeol P (2000) Extracellular ATP increases [CA(2+)](i) in distal tubule cells. I. Evidence for a P2Y2 purinoceptor. American journal of physiology Renal physiology 279 (1):F92-F101
6. Burnstock G (2007) Physiology and pathophysiology of purinergic neurotransmission. Physiological reviews 87 (2):659-797. doi:10.1152/physrev.00043.2006
7. Bustin SA, Benes V, Garson JA, Hellemans J, Huggett J, Kubista M, Mueller R, Nolan T, Pfaffl MW, Shipley GL, Vandesompele J, Wittwer CT (2009) The MIQE guidelines: minimum information for publication of quantitative real-time PCR experiments. Clinical chemistry 55 (4):611-622. doi:10.1373/clinchem.2008.112797
8. Dai LJ, Kang HS, Kerstan D, Ritchie G, Quamme GA (2001) ATP inhibits Mg(2+) uptake in MDCT cells via P2X purinoceptors. American journal of physiology Renal physiology 281 (5):F833-840
9. Ellison DH, Brooks VL (2011) Renal nerves, WNK4, glucocorticoids, and salt transport. Cell metabolism 13 (6):619-620. doi:10.1016/j.cmet.2011.05.007
10. Fuchs S, Philippe J, Corvol P, Pinet F (2003) Implication of Ref-1 in the repression of renin gene transcription by intracellular calcium. Journal of hypertension 21 (2):327-335. doi:10.1097/01.hjh.0000052414.12292.ef
11. Gailly P (1998) Ca2+ entry in CHO cells, after Ca2+ stores depletion, is mediated by arachidonic acid. Cell calcium 24 (4):293-304
12. Gesek FA, Friedman PA (1992) Mechanism of calcium transport stimulated by chlorothiazide in mouse distal convoluted tubule cells. The Journal of clinical investigation 90 (2):429-438. doi:10.1172/JCI115878
13. Gitelman HJ, Graham JB, Welt LG (1966) A new familial disorder characterized by hypokalemia and hypomagnesemia. Transactions of the Association of American Physicians 79:221-235
14. Gordon JL (1986) Extracellular ATP: effects, sources and fate. The Biochemical journal 233 (2):309-319
15. Ikura M, Osawa M, Ames JB (2002) The role of calcium-binding proteins in the control of transcription: structure to function. BioEssays : news and reviews in molecular, cellular and developmental biology 24 (7):625-636. doi:10.1002/bies.10105
16. Kaplan B, Davydov O, Knight H, Galon Y, Knight MR, Fluhr R, Fromm H (2006) Rapid transcriptome changes induced by cytosolic Ca2+ transients reveal ABRE-related sequences as Ca2+-responsive cis elements in Arabidopsis. The Plant cell 18 (10):2733-2748. doi:10.1105/tpc.106.042713

17. Kishore BK, Ginns SM, Krane CM, Nielsen S, Knepper MA (2000) Cellular localization of P2Y(2) purinoceptor in rat renal inner medulla and lung. American journal of physiology Renal physiology 278 (1):F43-51
18. Klar J, Sigl M, Obermayer B, Schweda F, Kramer BK, Kurtz A (2005) Calcium inhibits renin gene expression by transcriptional and posttranscriptional mechanisms. Hypertension 46 (6):1340-1346. doi:10.1161/01.HYP.0000192025.86189.46
19. Lazarowski ER, Boucher RC, Harden TK (2003) Mechanisms of release of nucleotides and integration of their action as P2X- and P2Y-receptor activating molecules. Molecular pharmacology 64 (4):785-795. doi:10.1124/mol.64.4.785
20. Lazarowski ER, Harden TK (1999) Quantitation of extracellular UTP using a sensitive enzymatic assay. British journal of pharmacology 127 (5):1272-1278. doi:10.1038/sj.bjp.0702654
21. Lazarowski ER, Rochelle LG, O'Neal WK, Ribeiro CM, Grubb BR, Zhang V, Harden TK, Boucher RC (2001) Cloning and functional characterization of two murine uridine nucleotide receptors reveal a potential target for correcting ion transport deficiency in cystic fibrosis gallbladder. The Journal of pharmacology and experimental therapeutics 297 (1):43-49
22. Lehrmann H, Thomas J, Kim SJ, Jacobi C, Leipziger J (2002) Luminal P2Y2 receptor-mediated inhibition of Na+ absorption in isolated perfused mouse CCD. Journal of the American Society of Nephrology : JASN 13 (1):10-18
23. Leipziger J (2003) Control of epithelial transport via luminal P2 receptors. American journal of physiology Renal physiology 284 (3):F419-432. doi:10.1152/ajprenal.00075.2002
24. Livak KJ, Schmittgen TD (2001) Analysis of relative gene expression data using real-time quantitative PCR and the 2(-Delta Delta C(T)) Method. Methods 25 (4):402-408. doi:10.1006/meth.2001.1262
25. Lu M, MacGregor GG, Wang W, Giebisch G (2000) Extracellular ATP inhibits the small-conductance K channel on the apical membrane of the cortical collecting duct from mouse kidney. The Journal of general physiology 116 (2):299-310
26. MacKenzie S, Vaitkevicius H, Lockette W (2001) Sequencing and characterization of the human thiazide-sensitive Na-Cl cotransporter (SLC12A3) gene promoter. Biochemical and biophysical research communications 282 (4):991-1000. doi:10.1006/bbrc.2001.4673
27. Misquitta C.M. CT, Grover A.K. (2006) Control of protein expression through mRNA stability in calcium signalling. Cell calcium 40 (4):329-346
28. Naveh-Many T, Nechama M (2007) Regulation of parathyroid hormone mRNA stability by calcium, phosphate and uremia. Current opinion in nephrology and hypertension 16 (4):305-310. doi:10.1097/MNH.0b013e3281c55ede

29. Olinger E, Schwaller B, Loffing J, Gailly P, Devuyst O (2012) Parvalbumin: calcium and magnesium buffering in the distal nephron. Nephrol Dial Transplant 27(11):3988-94. doi: 10.1093/ndt/gfs457.

30. Pochynyuk O, Bugaj V, Rieg T, Insel PA, Mironova E, Vallon V, Stockand JD (2008) Paracrine regulation of the epithelial Na+ channel in the mammalian collecting duct by purinergic P2Y2 receptor tone. The Journal of biological chemistry 283 (52):36599-36607. doi:10.1074/jbc.M807129200

31. Pochynyuk O, Rieg T, Bugaj V, Schroth J, Fridman A, Boss GR, Insel PA, Stockand JD, Vallon V (2010) Dietary Na+ inhibits the open probability of the epithelial sodium channel in the kidney by enhancing apical P2Y2-receptor tone. FASEB journal : official publication of the Federation of American Societies for Experimental Biology 24 (6):2056-2065. doi:10.1096/fj.09-151506
32. Pusl T, Wu JJ, Zimmerman TL, Zhang L, Ehrlich BE, Berchtold MW, Hoek JB, Karpen SJ, Nathanson MH, Bennett AM (2002) Epidermal growth factor-mediated activation of the ETS domain transcription factor Elk-1 requires nuclear calcium. The Journal of biological chemistry 277 (30):27517-27527. doi:10.1074/jbc.M203002200
33. Rieg T, Bundey RA, Chen Y, Deschenes G, Junger W, Insel PA, Vallon V (2007) Mice lacking P2Y2 receptors have salt-resistant hypertension and facilitated renal Na+ and water reabsorption. FASEB journal : official publication of the Federation of American Societies for Experimental Biology 21 (13):3717-3726. doi:10.1096/fj.07-8807com
34. Ross J (1995) mRNA stability in mammalian cells. Microbiological reviews 59 (3):423-450
35. Rozen S, Skaletsky H (2000) Primer3 on the WWW for general users and for biologist programmers. Methods in molecular biology 132:365-386
36. Sachs AB (1993) Messenger RNA degradation in eukaryotes. Cell 74 (3):413-421
37. Schaefer A, Magocsi M, Stocker U, Fandrich A, Marquardt H (1996) Ca2+/calmodulin-dependent and -independent down-regulation of c-myb mRNA levels in erythropoietin-responsive murine erythroleukemia cells. The role of calcineurin. The Journal of biological chemistry 271 (23):13484-13490
38. Schwiebert EM (2001) ATP release mechanisms, ATP receptors and purinergic signalling along the nephron. Clinical and experimental pharmacology & physiology 28 (4):340-350
39. Sorensen MV, Grossmann S, Roesinger M, Gresko N, Todkar AP, Barmettler G, Ziegler U, Odermatt A, Loffing-Cueni D, Loffing J (2013) Rapid dephosphorylation of the renal sodium chloride cotransporter in response to oral potassium intake in mice. Kidney international 83 (5):811-824. doi:10.1038/ki.2013.14
40. Taboubi S, Milanini J, Delamarre E, Parat F, Garrouste F, Pommier G, Takasaki J, Hubaud JC, Kovacic H, Lehmann M (2007) G alpha(q/11)-coupled P2Y2 nucleotide receptor inhibits human keratinocyte spreading and migration. FASEB journal : official publication of the Federation of American Societies for Experimental Biology 21 (14):4047-4058. doi:10.1096/fj.06-7476com
41. Taniyama Y, Sato K, Sugawara A, Uruno A, Ikeda Y, Kudo M, Ito S, Takeuchi K (2001) Renal tubule-specific transcription and chromosomal localization of rat thiazide-sensitive Na-Cl cotransporter gene. The Journal of biological chemistry 276 (28):26260-26268. doi:10.1074/jbc.M101614200
42. Unwin RJ, Bailey MA, Burnstock G (2003) Purinergic signaling along the renal tubule: the current state of play. News in physiological sciences : an international journal of physiology produced jointly by the International Union of Physiological Sciences and the American Physiological Society 18:237-241
43. Vallon V (2008) P2 receptors in the regulation of renal transport mechanisms. American journal of physiology Renal physiology 294 (1):F10-27. doi:10.1152/ajprenal.00432.2007

44. Vallon V, Rieg T (2011) Regulation of renal NaCl and water transport by the ATP/UTP/P2Y2 receptor system. American journal of physiology Renal physiology 301 (3):F463-475. doi:10.1152/ajprenal.00236.2011
45. Vargas-Poussou R, Dahan K, Kahila D, Venisse A, Riveira-Munoz E, Debaix H, Grisart B, Bridoux F, Unwin R, Moulin B, Haymann JP, Vantyghem MC, Rigothier C, Dussol B, Godin M, Nivet H, Dubourg L, Tack I, Gimenez-Roqueplo AP, Houillier P, Blanchard A, Devuyst O, Jeunemaitre X (2011) Spectrum of mutations in Gitelman syndrome. Journal of the American Society of Nephrology : JASN 22 (4):693-703. doi:10.1681/ASN.2010090907
46. Zambon AC, Hughes RJ, Meszaros JG, Wu JJ, Torres B, Brunton LL, Insel PA (2000) P2Y(2) receptor of MDCK cells: cloning, expression, and cell-specific signaling. American journal of physiology Renal physiology 279 (6):F1045-1052

Table 1. Primers used in real-time RT-PCR analyses.

Gene (Protein)	Forward and Reverse Primers	Amplimer length (bp)	Efficiency	Expression in mDCT cells (Ct)
Slc12a3 (NCC)	5' CCTCCATCACCAACTCACCT 3' 5' AGGAGGAAGAGGACGACTC 3'	151	0.98	
Pvalb (PV)	5' GACGCCATTCTTCTGGAAAT 3' 5' ATACCCC CACTGCCCTAAAA 3'	136	0.99	
Trpm6 (TRPM6)	5' TCTTCCTTCGAGAGCCATCA 3' 5' TCCACCAGGATTGGAGTCAC 3'	156	1.01	
β- actin	5' CCTGAACCCCAAAGCTAACA 3' 5' CGTCACCAGAGTCCATGACA 3'	146	0.98	
P2ry1 (P2Y1)	5' ACCCTACCAGCCCTCATCTT 3' 5' CTGTACCTGTGTGCGCTGAT 3'	146	1.01	26.4 ± 0.15
P2ry2 (P2Y2)	5' CGTGCTCTACTTCGTCACCA 3' 5' GAAAAGGGCACAGCAAAAAG 3'	135	0.97	27.5 ± 0.06
P2ry4 (P2Y4)	5' CACATCACCCGCACAATTTA 3' 5' G TCCCCCGTGAACAGATAGA 3'	150	1.02	32.3 ± 0.3
P2ry 6 (P2Y6)	5' CGCTTTGTACGCTTCCTCTT 3' 5' TCCACACACTACCCAAGCAG 3'	150	1.09	27.5 ± 0.4
P2rx1 (P2X1)	5' ACTGGGAGTGTGACCTGGA 3' 5' AGAGGTGACGACGGTTTGTC 3'	150	0.99	33.9 ± 0.51
P2rx2 (P2X2)	5' CCATGTCGGAACACAAAGTG 3' 5' GGCAGGTAGAGCTGTGAAC 3'	153	0.95	32.9 ± 0.14
P2rx3 (P2X3)	5' GACACCGTGGAGATGCCTAT 3' 5' AT GGAAGCGGCACTTCTTTA 3'	147	0.97	34.1 ± 0.36
P2rx4 (P2X4)	5' CCTCGACACTCGGGACTTA 3' 5' GCCTTTCCAAACACGATGAT 3'	147	0.99	26.8 ± 0.13
P2rx5 (P2X5)	5' ACTTCCCTGCAGAGTGCTGT 3' 5' GGAGTCACGATCAGGTTGGT 3'	155	1.03	30.2 ± 0.37
P2rx6 (P2X6)	5' CCCAGAGCATCCTTCTGTTC 3' 5' CACCAGCTCCAGATCTCACA 3'	150	0.98	35.2 ± 0.34
P2rx7 (P2X7)	5' AAGCTGTACCAGCGGAAAGA 3' 5' CCTGCAAAGGGAAGGTGTAG 3'	152	0.97	33.5 ± 0.17
Gapdh	5' TGCACCACCAACTGCTTAGC 3' 5' GGATGCAGGGATGATGTTCT 3'	176	0.99	

Figure legends

Figure 1. Nucleotide stimulation of mDCT cells activates metabotropic P2 receptors and decreases NCC expression.

A. Repetitive stimulation with 10µM ATP/UTP induced a 2-fold decrease of NCC mRNA expression (RT-qPCR). (n=8). ***, p<0.0001 and a 40 % reduction in NCC protein expression (n=2 independent experiments, with beta-actin as control). **B**. Stimulation of mDCT cells with ATP/UTP induced Ca^{2+} transients. Representative recording of mDCT cells stimulated by ATP in the presence (2 mM $[Ca^{2+}]_e$; a) and ATP or UTP in the absence (0 mM $[Ca^{2+}]_e$; b and c) of extracellular calcium. ATP or UTP induces the release of $[Ca^{2+}]_i$ from internal stores (dark lines). Cells preincubated for 10 minutes with 10µM PLC inhibitor (U73122) lacked nucleotide-induced $[Ca^{2+}]_i$ transients (a-c; red lines). Similar results were obtained for n=3-11 in each condition. Stimulation with 10 µM and 100 µM UTP (panel d) induced a similar amplitude of $[Ca^{2+}]_i$ transient (n=4-5). The time points of drug stimulation are indicated by arrows **C**. P2 receptors expression in mDCT cells. **a.** RT-PCR analyses showed that $P2Y_1$, $P2Y_2$, P2X4 and $P2X_5$ are highly expressed in mDCT cells (see also Table 1). **b.** Immunofluorescence staining (confocal images in XZ plane) is compatible with a $P2Y_2$ receptor (green) expression in the apical membrane and a PV expression (red) in the cytosol.

Figure 2. Effects of $P2Y_2$ receptor knock-down on intracellular Ca^{2+} release and NCC mRNA expression in mDCT.

A. a. P2Y receptor mRNA expression in mDCT cells after transfection with three different si$P2Y_2$. $P2Y_1$ (white columns) $P2Y_2$ receptors (black columns) mRNAs were quantified by RT-qPCR, related to GAPDH expression and expressed in proportion to control situation (siCtrl). Cells treated with si$P2Y_2$ RNA showed a significant decrease in the expression of $P2Y_2$, whereas $P2Y_1$ stayed unchanged. ***, p < 0.0001 vs. siCtrl (n=4). Efficiency of transfection was around 90%, verified with BLOCK-iT™ Alexa Fluor® Red Fluorescent Oligo (Invitrogen). b. Immunoblot analysis of $P2Y_2$ protein expression of cells transfected with si$P2Y_2$ *vs* siCtrl.

B. Specific $P2Y_2$ receptor knock-down inhibits intracellular Ca^{2+} release in mDCT. a. Representative recording of changes in $[Ca^{2+}]_i$ measured with the fluorescent indicator Fura2-AM. Stimulation of mDCT cells with 10 µM UTP induced a release of Ca^{2+} in the

absence of $[Ca^{2+}]_e$ after siCtrl treatment (dark line) but not after transfection with $siP2Y_2$, (red-line). The time point of drug stimulation is indicated by arrow. b. Quantification (n=6 independent measurements; ***: p < 0.0001).

C. Stimulation with 10µM UTP for 10 min every hour for 6 hours induced a 2-fold decrease of NCC expression (RT-qPCR), an effect that was blocked after $P2Y_2$ silencing (n = 8, **: $p < 0.001$)

Figure 3. Cytoplasmic overexpression of PV modulates $[Ca^{2+}]_i$ transients and NCC expression induced by nucleotide stimulation

A. *Subcellular localization of targeted PV-GFP fusion proteins.* Schematic representation of PV-GFP expression vectors and fluorescent detection (green) of PV-GFP fusion proteins targeted to the cytoplasm (PV-cyt and PV-cyt-CDEF) or to the nucleus (PV-nuc). Nuclei stained with DAPI dye (blue).

B. *Overexpression of PV-cyt but not of PV-cyt-CDEF or PV-nuc decreases $[Ca^{2+}]_i$ response to 10 µM UTP.* a. Representative recording of $[Ca^{2+}]_i$ transients of cells transfected with PV-cyt (black line), PV-cyt-CDEF (red line) or PV-nuc (green line). b. Quantification (mean ± sem, n=19-40, ***: $p < 0.001$).

C. *Overexpression of PV-cyt inhibits UTP-induced decrease of NCC expression.* mDCT cells were transfected with Mock and PV-cyt, PV-cyt-CDEF and PV-nuc constructs and treated after 72 hours with 10 µM UTP for 10 minutes every hour for 6 hours. NCC expression was measured by RT-qPCR (mean ± sem, n=6-25; **: $p<0.001$; ***: $p<0.0001$).

Figure 4. Nucleotide stimulation does not affect NCC gene transcription.

A. Luciferase reporter constructs containing 1-kb, 1.5-kb and 2.2-kb fragments of promoter of the mouse *Slc12a3* gene coding for NCC. **B.** Luciferase activity was assessed after 24 hours by Dual-Luciferase Assay in cells that were stimulated with 10 µM UTP for 10 minutes every hour for 6 hours. Firefly luciferase activity corrected for transfection efficiency by relating to *Renilla* luciferase measurements and related to the corrected activity of the promoterless pGL3-basic activity (mean ± sem, n=4 independent measurements).

Figure 5. Nucleotide stimulation decreases NCC mRNA half-life time in mDCT cells.

mDCT cells were incubated with 75µM DRB for 0, 1, 3, 6 and 9 hours and stimulated with 10 µM UTP for 10 minutes every hour for 6 hours. NCC, β-actin and TRPM6 mRNAs were quantified by RT-qPCR (mean ± sem, n=4-11 independent experiments).

Figure

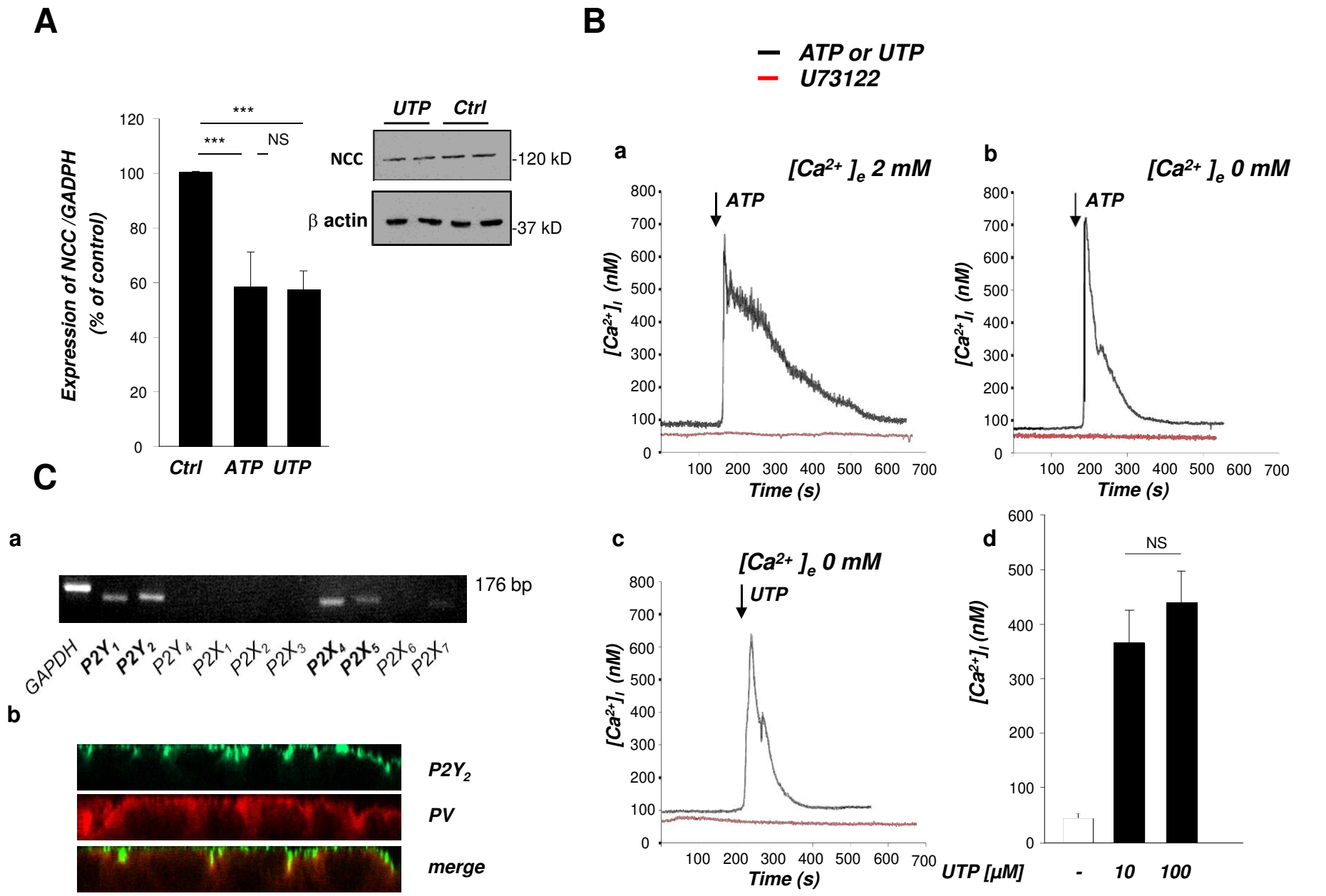
A
Expression of NCC /GADPH (% of control)
120
100
80
60
40
20
0
***
***
NS
Ctrl
ATP
UTP
UTP
Ctrl
NCC
-120 kD
β actin
-37 kD
B
ATP or UTP
U73122
a
[Ca2+]e 2 mM
ATP
[Ca2+]I (nM)
Time (s)
b
[Ca2+]e 0 mM
ATP
c
[Ca2+]e 0 mM
UTP
d
NS
[Ca2+]I (nM)
UTP [μM]
-
10
100
C
a
176 bp
GAPDH
P2Y1
P2Y2
P2Y4
P2X1
P2X2
P2X3
P2X4
P2X5
P2X6
P2X7
b
P2Y2
PV
merge

Fig. 1

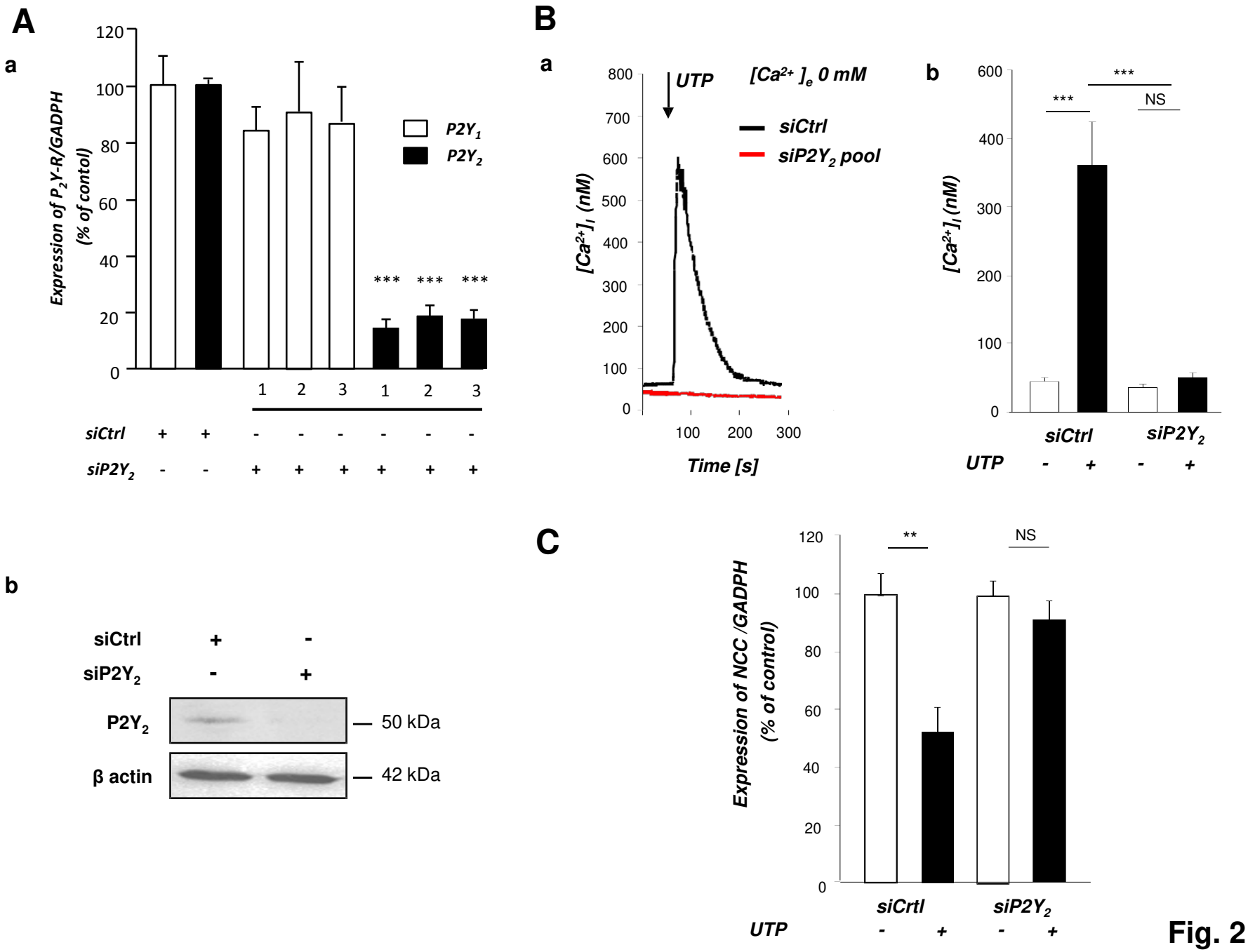
A
a
Expression of P2Y-R/GADPH (% of contol)
120
100
80
60
40
20
0
P2Y1
P2Y2
***
***
***
1 2 3 1 2 3
siCtrl + + - - - - - -
siP2Y2 - - + + + + + +
b
siCtrl + -
siP2Y2 - +
P2Y2
50 kDa
β actin
42 kDa
B
a
UTP
[Ca2+]e 0 mM
siCtrl
siP2Y2 pool
[Ca2+]i (nM)
800
700
600
500
400
300
200
100
0
100 200 300
Time [s]
b
[Ca2+]i (nM)
600
400
300
200
100
0
***
***
NS
siCtrl
siP2Y2
UTP - + - +
C
Expression of NCC /GADPH (% of control)
120
100
80
60
40
20
0
**
NS
siCrtl
siP2Y2
UTP - + - +

Fig. 2

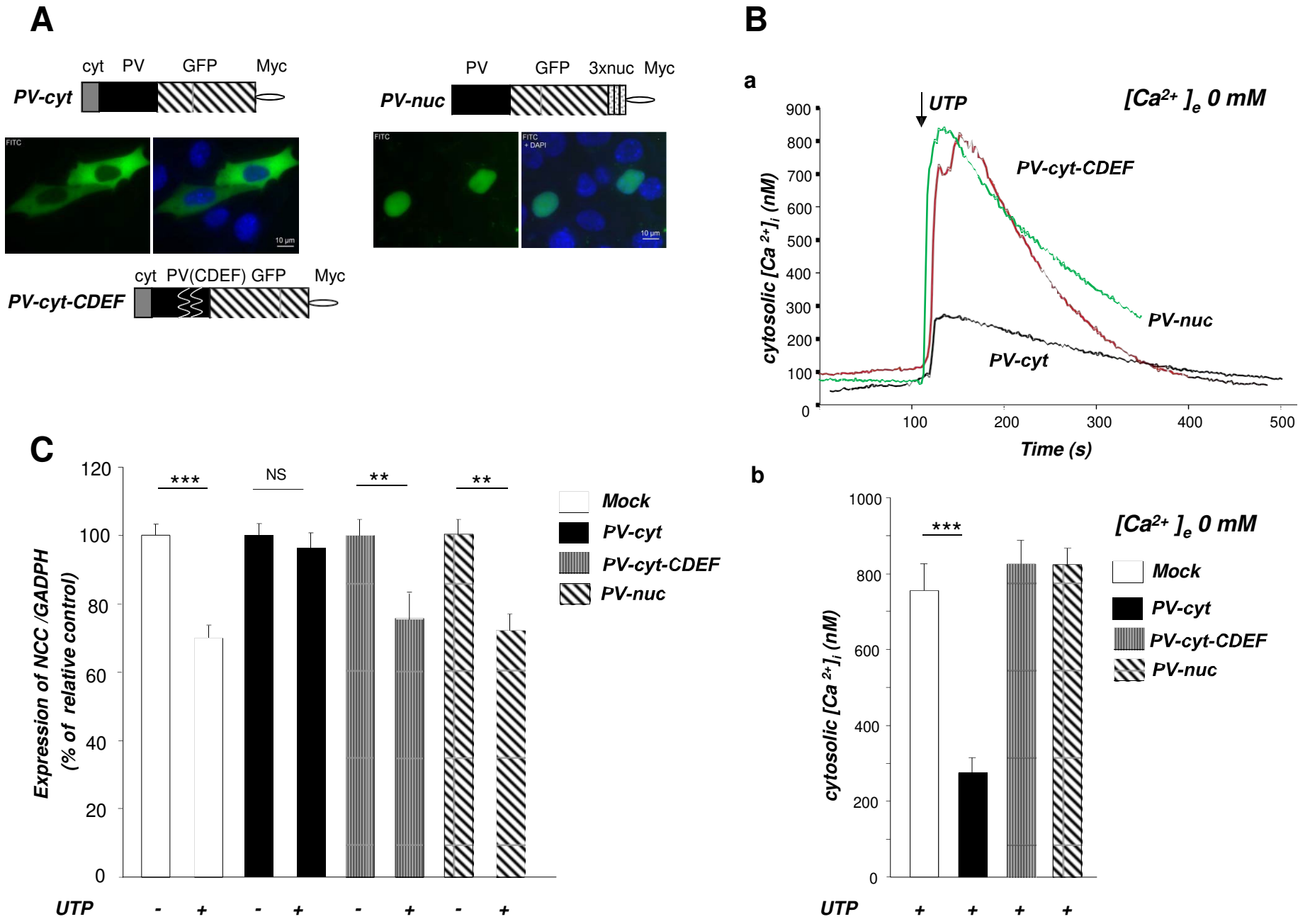
A
cyt PV GFP Myc
PV-cyt
PV GFP 3xnuc Myc
PV-nuc
cyt PV(CDEF) GFP Myc
PV-cyt-CDEF
B
a
UTP
[Ca2+]e 0 mM
PV-cyt-CDEF
PV-nuc
PV-cyt
cytosolic [Ca 2+]i (nM)
Time (s)
b
[Ca2+]e 0 mM
Mock
PV-cyt
PV-cyt-CDEF
PV-nuc
cytosolic [Ca 2+]i (nM)
UTP
C
Expression of NCC /GADPH
(% of relative control)
***
NS
**
**
Mock
PV-cyt
PV-cyt-CDEF
PV-nuc
UTP

Fig. 3

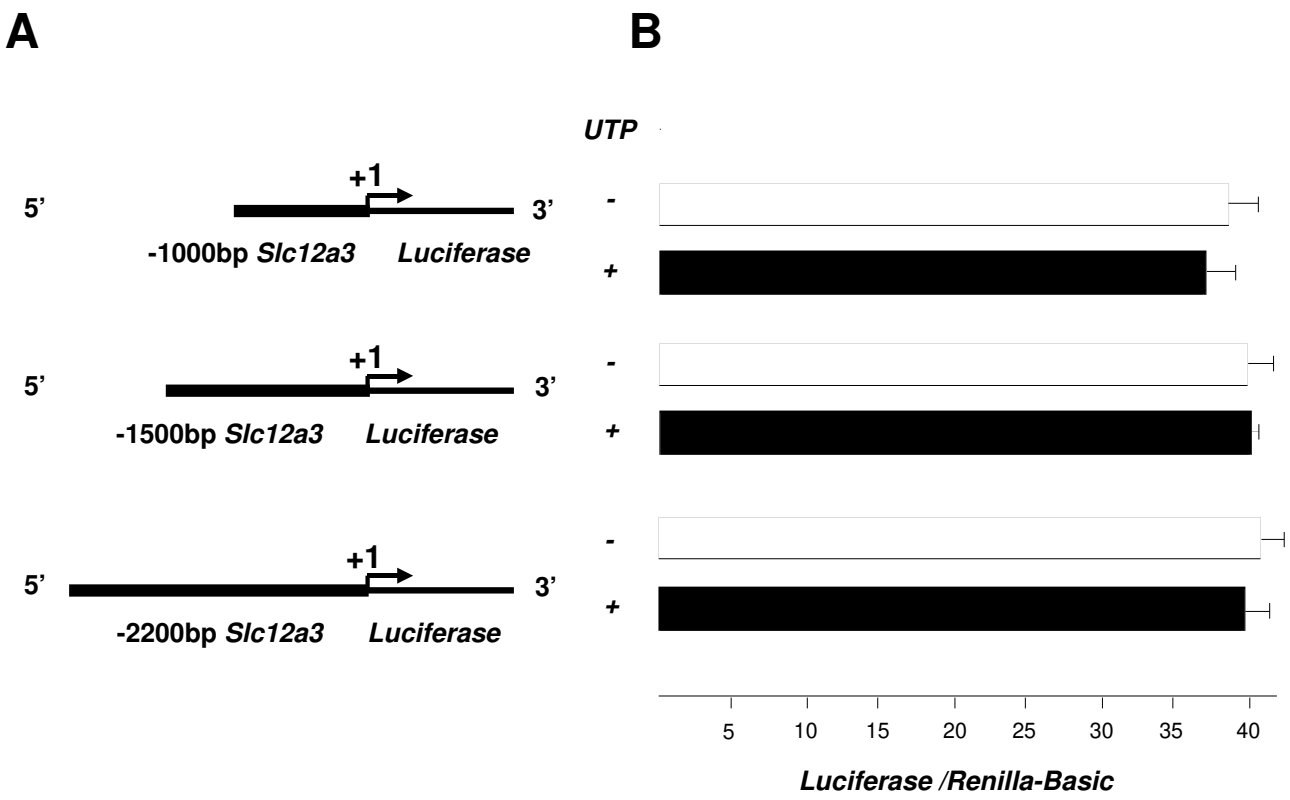
A
B
UTP
+1
5'
3'
-1000bp Slc12a3
Luciferase
-1500bp Slc12a3
Luciferase
-2200bp Slc12a3
Luciferase
-
+
5
10
15
20
25
30
35
40
Luciferase /Renilla-Basic

Fig. 4

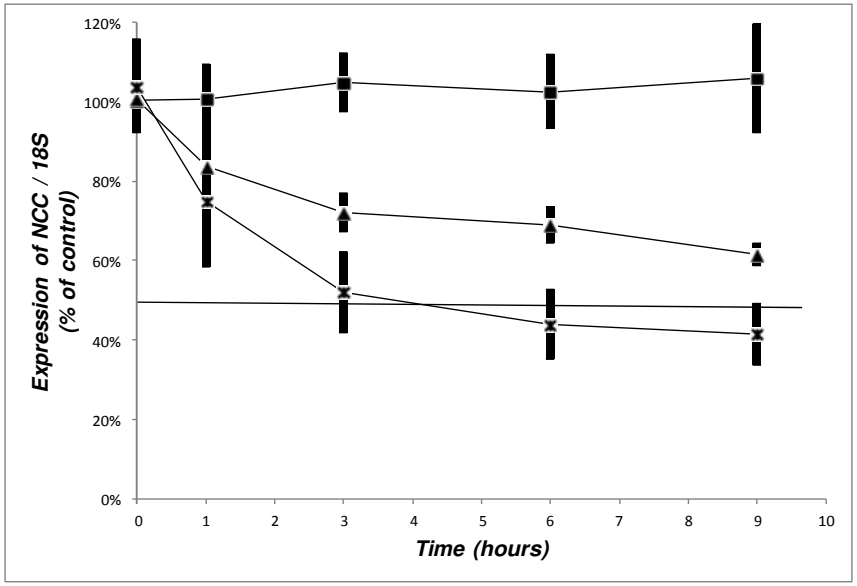
120%
100%
80%
60%
40%
20%
0%
0 1 2 3 4 5 6 7 8 9 10
Expression of NCC / 18S (% of control)
Time (hours)

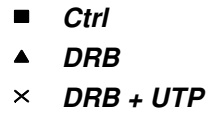
Ctrl
DRB
DRB + UTP

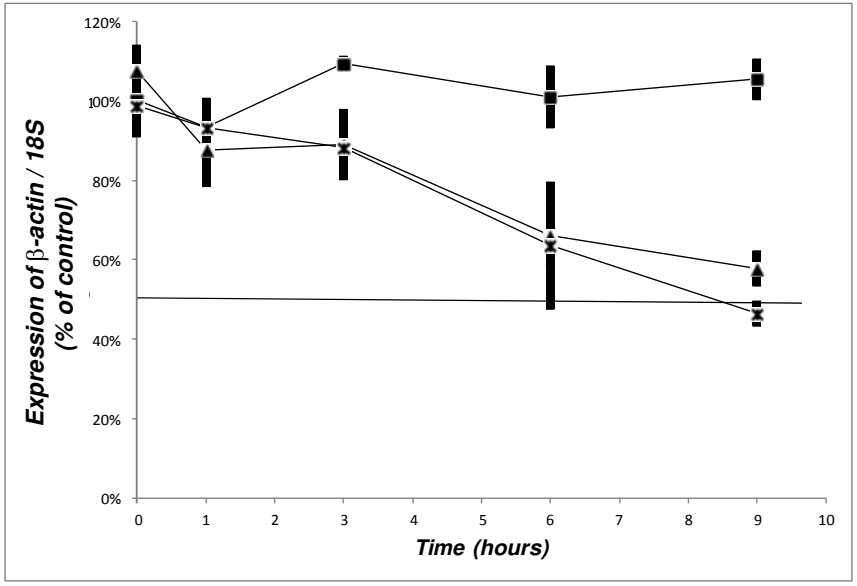
120%
100%
80%
60%
40%
20%
0%
0 1 2 3 4 5 6 7 8 9 10
Expression of β-actin / 18S (% of control)
Time (hours)

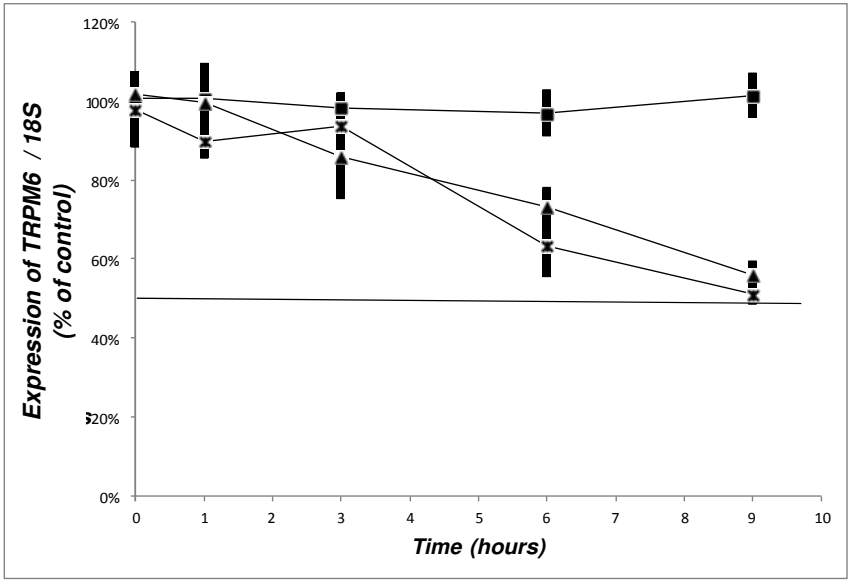
120%
100%
80%
60%
40%
20%
0%
0 1 2 3 4 5 6 7 8 9 10
Expression of TRPM6 / 18S (% of control)
Time (hours)

Fig. 5